CrossMark

Sertoli Cells Avert Neuroinflammation-Induced Cell Death and Improve Motor Function and Striatal Atrophy in Rat Model of Huntington Disease

Houssein Ahmadi[1] · Mahdi Eskandarian Boroujeni[2] · Yousef Sadeghi[1] · Mohammad Amin Abdollahifar[1] · Fariba Khodagholi[3] · Gholam Houssein Meftahi[4] · Mohammadmehdi Hadipour[4] · Amir-Hossein Bayat[5] · Fatemeh Shaerzadeh[6] · Abbas Aliaghaei[1]

Abstract

Huntington's disease (HD) is a genetically heritable disorder, linked with continuing cell loss and degeneration mostly in the striatum. Currently, cell therapy approaches in HD have essentially been focused on replenishing or shielding cells lost over the period of the disease. Herein, we sought to explore the in vitro and in vivo efficacy of primary rat Sertoli cells (SCs) and their paracrine effect against oxidative stress with emphasis on HD. Initially, SCs were isolated and immunophenotypically characterized by positive expression of GATA4. Besides, synthesis of neurotrophic factors of glial cell-derived neurotrophic factor and VEGF by SCs were proved. Next, PC12 cells were exposed to hydrogen peroxide in the presence of conditioned media (CM) collected from SC (SC-CM) and cell viability and neuritogenesis were determined. Bilateral striatal implantation of SC in 3-nitropropionic acid (3-NP)-lesioned rat models was performed, and 1 month later, post-graft analysis was done. According to our in vitro results, the CM of SC protected PC12 cells against oxidative stress and remarkably augmented cell viability and neurite outgrowth. Moreover, grafted SCs survived, exhibited decreases in both gliosis and inflammatory cytokine levels, and ameliorated motor coordination and muscle activity, together with an increase in striatal volume as well as in dendritic length of the striatum in HD rats. In conclusion, our results indicate that SCs provide a supportive environment, with potential therapeutic benefits aimed at HD.

Keywords Transplantation · Huntington · Striatum · Sertoli cells · Neuroprotection

Introduction

Huntington's disease (HD) is a heritable disorder, genetically instigated by insertion mutation of huntingtin gene (*Htt*), linked with continuing cell loss and degeneration mostly in the striatum and neocortex (Bates et al. 2014; Leegwater-Kim and Cha 2004; MacDonald et al. 1993). Currently, cell therapy approaches in HD have essentially been focused on replenishing or shielding cells lost over the period of the disease (Clelland et al. 2008). Sertoli cells (SCs) as the nurturing cells are located within seminiferous tubules of the testis and provide an immunoprivileged milieu for the growing spermatogonia. SCs have been demonstrated to locally immunoprotect co-implanted cells (Shamekh et al. 2006; Korbutt et al. 1997; Sanberg et al. 1996; Suarez-Pinzon et al. 2000; Yang et al. 2002; Willing et al. 1999a), improve cell proliferation and neuronal induction (Shamekh et al. 2008; Hemendinger et al. 2005), and survive for prolonged periods of time once grafted (Dufour et al. 2008). Prior works have

✉ Abbas Aliaghaei
aghaei60@gmail.com

1 Department of Cell Biology and Anatomical Sciences, School of Medicine, Shahid Beheshti University of Medical Sciences, Tehran, Iran

2 Department of Stem Cells and Regenerative Medicine, Faculty of Medical Biotechnology, National Institute of Genetic Engineering and Biotechnology, Tehran, Iran

3 Neuroscience Research Center, Shahid Beheshti University of Medical Sciences, Tehran, Iran

4 Neuroscience Research Center, Baqiyatallah University of Medical Sciences, Tehran, Iran

5 Department of Neuroscience, Saveh University of Medical Sciences, Saveh, Iran

6 Department of Neuroscience, McKnight Brain Institute, University of Florida College of Medicine, Gainesville, FL 32611, USA

implemented isolated SCs for the remedy of diseases in animal models, namely diabetes and Parkinson's disease (PD) (Suarez-Pinzon et al. 2000; Willing et al. 1999a). Moreover, SCs are capable of secretion of plenty of immunoregulatory and trophic factors including Fas (CD95) ligand (FasL), transforming growth factors (TGF-α and TGF-β), interleukin 1α (IL-1α) and interleukin 6 (IL-6), platelet-derived growth factor (PDGF), and neurturin (NTN) (Piccirillo et al. 1998; Griswold 1993; Skinner 1993; Gnessi et al. 1995; French et al. 1996; Widenfalk et al. 1997; Cudicini et al. 1997; Sanberg et al. 1997b; O'Bryan et al. 2005). Regarding the central nervous system, SCs grafted into the brain and spinal cord could deliver compounds with trophic and anti-inflammatory effects on the neighboring environment (Borlongan et al. 1997).

Past study has shown that SC transplants were able to reverse locomotor anomalies in a 3-nitropropionic acid (3-NP) model of early HD. Besides, there is growing evidence to imply that injection of growth factors prior or just after the promotion of denervation in animal models could abate neuronal atrophy (Rodriguez et al. 2003; Emerich 2003). The current study was designed to investigate the in vitro and in vivo efficacy of primary rat SCs and their paracrine effect against oxidative stress with emphasis on HD.

Materials and Methods

Isolation and Culture of Sertoli Cells

Under approval by the animal care committee of Shahid Beheshti University of Medical Sciences, male albino Wistar rats (20–30 days old) were killed under deep anesthesia and the testes were removed. The tunica albuginea was removed from the individual testis, and the tissue was sequentially digested first with trypsin (0.25%) for 15 min and then with collagenase (0.1%) for 15 min at 37 °C. Afterwards, fetal bovine serum (FBS) was added, and after centrifugation of the solution, the pellet was transferred to a culture media containing DMEM/F12 and FBS (10%). Forty-eight hours later, the culture media was changed in order to discard the debris and red blood cells. For collecting the conditioned media of SC (SC-CM), SC was cultured in serum-free medium. After 48 h, medium was collected, filtered, and kept at − 20 °C for future uses.

Immunocytofluorescence

Sertoli cells were cultured in a 24-well plate and fixed by 4% paraformaldehyde (PFA). After washing with PBS, cells were permeabilized with Triton X-100. Then, cells were incubated with goat normal serum followed by an overnight incubation with the primary antibody against GATA4 at 4 °C. The fluorescent secondary antibody was applied after washing with PBS. For visualization of the nuclei, cells were stained by DAPI. Preparations were examined under a fluorescent microscope (Olympus IX71, Japan).

PC12 Cell Culture and Treatment

PC12 cells were obtained from the Institute of Pasture (Iran, Tehran). The cells were cultured in DMEM/F12 media supplemented with 10% FBS and penicillin and streptomycin (1%). Then, PC12 cells were treated with SC-CM (4:1 ratio of SC-CM to DMEM/F12 medium) and simultaneously exposed to H_2O_2 (150 μM) for 24 h.

Examination of PC12 Cell Morphology

PC12 cells were seeded in six-well plates. For morphological analysis, random images were acquired from each well, taking 20 images per well. A minimum of 50 cells per treatment was quantified. After co-administration of SC-CM and H_2O_2, neurite length was assessed. Neurite length was defined as the sum of lengths of all primary branches and their associated twigs. Data analysis was done by using the Cell^A program.

3-(4,5-Dimethylthiazol-2-yl)-2,5-diphenyltetrazolium bromide Assay

PC12 cells were cultured in a 96-well plate. After treatment, 3-(4,5-dimethylthiazol-2-yl)-2,5-diphenyltetrazolium bromide (MTT) was added to each well and incubated for 4 h. Then, the supernatant was removed and dark blue crystal of formazan was dissolved in dimethyl sulfoxide. Absorption of the suspension was read at 630 nm, and the measurements were reported as a percentage of control.

Cell Viability Assay

Living and dead cells were distinguished using the Eukolight™ viability/cytotoxicity assay (Molecular Probes). Culture medium was replaced with 2 mM calcein acetoxymethyl ester and 4 mM ethidium homodimer-1. Viable (green fluorescent by calcein) and non-viable (red fluorescent by ethidium) PC12 cells present in 10–20 random microscopic fields per condition per experiment were recorded.

3-NP Toxicity Model

Thirty male Sprague Dawley rats (200–220 g body weight at the beginning of the study) were used. Rats were housed at 22 °C, under 12 h light/12 h dark conditions with ad libitum access to food and water. Besides, after post cell transplantation and post electromyography, an analgesic (buprenorphine hydrochloride, 0.1 ml of 0.3 mg/ml) was subcutaneously injected. Twenty rats were randomly assigned into two groups

that were treated with 3-NP during 5 days, and 10 control rats were given vehicle (phosphate-buffered saline, PBS). In the 3-NP groups, all animals received intraperitoneal (i.p.) 3-NP (30 mg/kg) injections once daily for five consecutive days.

SC Transplantation

Bilateral cell transplantation was performed 7 days after the beginning of 3-NP administration. The animals were assigned to one of three experimental groups: control or intact groups (n = 10), 3-NP + vehicle (n = 10), and Sertoli cells + 3-NP (250,000 cells; n = 10). The SC was maintained alive in suspension using a 2-μl DMEM aliquot, stored on ice during the surgery procedure. After being anesthetized (i.p.) with xylazine (10 mg/kg) and ketamine (75 mg/kg), the animals were bilaterally transplanted with SC in each striatum labeled with Hoechst 33258 (5 μg/ml) using a 5-μl Hamilton microsyringe placed at the following coordinates, relative to the bregma: + 0.5 mm AP, ±2.6 mm ML, and − 6 and − 5 mm DV. SC was transplanted in the part of the striatum (medio-posterior part) which was devoid of 3-NP-induced cell loss, in order to maximize graft survival. In the 3-NP group, rats received media as vehicle. Rats were sacrificed at 30 days post transplantation.

Rotarod Test

A behavioral test was performed 1 day before the injection of 3-NP, and at the 1st, 2nd, 3rd, and 4th week after the cell transplantation. Rats were placed on the accelerating cylinder at speeds increasing from 4 to 40 rpm over a 5-min test session. The test was stopped if the animal fell off the rungs or gripped the device and spun around for two consecutive revolutions without attempting to run. The maximum time that each animal remained on the device was recorded.

Electromyography

Animals were placed under general anesthesia via intraperitoneal injection of ketamine hydrochloride (60 mg/kg) and xylazine (8 mg/k). After that, the right hind limb of animal was shaved and cleaned with a Betadine solution. A 3-cm skin incision was made longitudinally on the posterior aspect of each thigh, from the greater trochanter to the knee. Then, dissection was performed between the gluteus maximus and biceps femoris muscles, and the sciatic nerve was exposed, along with the gastrocnemius muscle. With appearance of the sciatic nerve using forceps and, cautiously, in order to avoid damage to the nerve, it is separated from the surrounding connective tissue in which stimulation electrodes could able to pass under the sciatic nerve. For electrical stimulation, two monopolar subdermal Teflon needle electrodes were used, arranged in parallel at a fixed distance of 7 mm from each other. The recording electrodes had an insulating coating over, leaving the distal uncoated. The sciatic nerve was then stimulated (1 A, 0.2 Hz frequency, 100 s long), and the compound muscle action potential was recorded in the gastrocnemius muscle on the side ipsilateral to the stimulation. The compound muscle action potential parameters analyzed were amplitude and latency. Also during stimulation and recording, ringer solution was used in order to prevent drying of the nerve.

Western Blot

The animals were killed, their brains were removed, and the striatum was extracted. Tissues were lysed by tissue lysis buffer. To determine the protein concentration in the samples, the Bradford test was performed. Twenty micrograms of protein was loaded on 12% SDS-PAGE gel and electrophoresis followed by transfer onto PVDF. Then, blots were incubated with blocking solution followed by incubation with primary antibody against caspase-3 overnight. After being washed, blots were incubated with secondary antibody and, finally, immunoreactivity of polypeptides was detected using ECL solution. The absorbance of resulting bands was quantified by densitometry using ImageJ software. For detection of neurotrophic factors of glial cell-derived neurotrophic factor (GDNF) and VEGF, SC was lysed in lysis buffer containing a protease inhibitor and the abovementioned procedure was performed.

Immunohistochemistry

Rats were deeply anesthetized by chloral hydrate and perfused transcardially using chilled saline followed by a fixative consisting of 4% paraformaldehyde in 0.1 M PBS. Then, brains were placed in formalin, prepared, and placed on slides. The primary antibody was diluted with PBS containing 0.3% Triton X-100 and 1% bovine serum albumin (BSA). Sections were incubated in primary antibodies against GFAP (1:300) overnight in 4 °C. Sections were then incubated with the avidin–biotin complex substrate and treated with 0.05% 3,3-diaminobenzidine tetrahydrochloride and 0.03% hydrogen peroxide in 0.05 m Tris buffer (pH 7.6). After immunohistochemical reaction, sections were mounted, counterstained, and observed under a light microscope.

Estimation of the Striatum Volume

The rat's brain tissue samples were fixed in 10% formalin for 1 week. Following tissue processing, serial coronal sections of 10 μm thickness were prepared and stained with cresyl violet (0.1%). To measure the total volume of the striatum using Cavalieri's principle, the following formula was used:

$$V (striatum) = \sum P \times a/p \times t$$

Estimation of Total Length of Dendrite

The length of dendrite was estimated using the oriented cycloid. The striatum was cut into systematic uniform random sectioning. They were embedded in a paraffin block, sectioned (60 μm thickness), and stained with 1% silver nitrate. Mean dendritic length was calculated using the following formula:

$$I_n = \frac{Total\ dendritic\ length}{Total\ number\ of\ neurons}$$

To measure the length, a vertical section was considered. A cycloid grid and a counting frame were superimposed on the live images of the striatum. Using a microscope (Nikon E-200) equipped with an objective lens connected to a computer, the dendrite length per neuron was assessed; two values were measured: (i) the number (Q) of cell bodies of the neurons using the optical disector method and (ii) the total number of intersections (I) between the dendrite axes and the oriented cycloid. The following formula was used:

$$I_n = 2 \times \frac{a}{l} \times \frac{1}{asf} \times M^{-1} \times \frac{\sum Q}{\sum I}$$

where al is the test area per cycloid test length, asf is the area associated with the cycloid grid divided by the area of the counting frame, and M is the final magnification.

RNA Extraction and Complementary DNA Synthesis

Total RNA was extracted using High Pure RNA Isolation Kit, according to the manufacturer's instructions (Roche, Basel, Switzerland). Then, 1 μg of total RNA was transcribed to cDNA using murine leukemia virus (MuLV) reverse transcriptase (Fermentas, Lithuania) in the presence of random hexamers and RNase inhibitor.

Quantitative Real-Time PCR

Real-time quantitative PCR (qPCR) analysis was conducted using specific primers for interleukin 1 beta (IL-1β) and tumor necrosis factor alpha (TNF-α) genes. GAPDH was used as internal control (Table 1). Reactions were performed using SYBR® Premix Ex Taq™ II (Takara Bio, Inc.) on a Rotor-Gene™ 6000 real-time PCR machine (Corbett Research, Qiagen, Germany). Initial denaturation was performed at 95 °C for 15 min followed by 40 cycles of denaturation at 95 °C for 5 s, under primer-specific conditions (Table 1), and extension at 60 °C for 20 s. Comparative real-time qPCR quantitation was conducted between candidate groups using Relative Expression Software Tool (REST) 2009 (Qiagen).

Data Analysis

All data are represented as the mean ± SEM. Comparison between groups was made by one-way analysis of variance (ANOVA) followed by Tukey's multiple comparison test to analyze the difference. The statistical significances were achieved when $P < 0.05$.

Results

SC Exhibited Fibroblast-Like Morphology and Expressed Neurotrophic Factors of GDNF and VEGF

One week after SCs were cultured, fibroblast-like cells appeared in culture dishes. The cells grew rapidly and covered the surface (Fig. 1a). Immunocytochemistry analysis indicated that SC was immunopositive for GATA4 (Fig. 1b). To examine their ability for production of neurotrophic factors GDNF and VEGF, we detected these factors by western blot. Our data revealed that SC could express GDNF and VEGF (Fig. 1c).

SC-CM Precluded the Disruption of Neurite Outgrowth Induced by H_2O_2

In the next step, we evaluated neurite outgrowth in PC12 cells treated with SC-CM and H_2O_2 simultaneously after 24 h (Fig. 2a, b). Accordingly, neurite length in the group that received H_2O_2 and SC-CM was 1.51-fold higher than H_2O_2-treated cells.

SC-CM Protected PC12 Cells Against H_2O_2-Induced Cell Death

To assess the effect of SC-CM on the survival of PC12 cells, live and dead assay was performed. The dead cells (red fluorescent) and live PC12 cells (green fluorescent) under oxidative stress are shown in Fig. 3a. Viability of cells treated with SC-CM and H_2O_2 was determined by the MTT assay. As displayed in Fig. 3b, MTT assay revealed that cell viability 24 h after the presence of SC-CM and H_2O_2 increased significantly compared to the cells incubated only with H_2O_2 (Fig. 3b).

Transplantation of SC in Rats Pre-treated with 3-NP Augmented Motor Coordination and Muscle Activity

To evaluate whether the transplantation of SC in the rat striatum improved the coordination of movement after injection of 3-NP and vehicle, the rotarod test was performed. Motor coordination was significantly decreased in the 3-NP-receiving vehicle group in comparison with the control group. However, after transplant of SC, motor coordination of the SC + 3-NP group was considerably higher than that of the 3-NP-receiving vehicle animals.

Table 1 Quantitative real-time PCR primers list

Primer name		Sequence	Annealing	Accession
GAPDH	F	GAACATCATCCCTGCATCCA	60 °C × 25 s	NM_017008.4
	R	GCCAGTGAGCTTCCCGTTCA		
IL-1β	F	AAAGAAGAAGATGGAAAAGCGGTT	60 °C × 25 s	NM_031512.2
	R	GGGAACTGTGCAGACTCAAACTC		
TNF-α	F	ACCACGCTCTTCTGTCTACTG	60 °C × 25 s	NM_012675.3
	R	CTTGGTGGTTTGCTACGAC		

Following the injection of SC, the coordination of movement enhanced over the 4-week period ($P < 0.05$) (Fig. 4).

To measure the efficacy of SC transplantation on muscle activity, the electromyography (EMG) was performed (Fig. 5a). Latency demonstrated an increase in the 3-NP-receiving vehicle group in contrast to the control group. Following grafting of SC, latency declined in the SC + 3-NP compared with the 3-NP group (Fig. 5b).

Transplant of SC in the 3-NP Group Decreased Apoptosis

After transplant of SC in 3-NP-injected rats, western blotting analysis unveiled that cleaved caspase-3 in the 3-NP-injected rats was 3.67-fold higher than that in the control group. Nonetheless, cleavage of caspase-3 in the group which received SC was approximately 1.4 times lower compared to that in 3-NP-injected ones (Fig. 6a, b).

SC Implantation in Rats with 3-NP Boosted the Total Length of Dendrite

Following the injection of SC into the striatum of rats, our results confirmed that these cells survived in the brain after 30 days (Fig. 7a, b). Besides, silver staining of striatal medium spiny neuron (MSN) illustrated that the striatum of the SC + 3-NP group had higher dendritic length contrary to the 3-NP group ($P < 0.05$) (Fig. 8a, b).

Grafted SC in 3-NP-Lesioned Rats Declined Gliosis

For detection of astrocyte migration (gliosis), immunohisto-chemistry against GFAP was done. Migration of astrocytes in the 3-NP group was statistically higher than that in the control. In the group receiving SC, the number of astrocytes exhibited a significant drop compared with the 3-NP group (Fig. 9a, b).

Transplantation of SC Improved Striatal Volume in HD Rats

Our stereological analysis showed grafted SC attenuated the atrophy of striatal volume. The results disclosed that the volume of the striatum was decreased in the 3-NP group in comparison to the control group ($P < 0.001$). But, striatal volume showed an increase in the SC + 3-NP contrary to the 3-NP lesioned group ($P < 0.01$) (Fig. 10a, b).

Fig. 1 Culture expansion and in vitro characterization of SC. **a** Fibroblast-like morphology of SC after 1 week of isolation. Scale bar = 200 μm. **b** Immunocytochemical staining indicated that SCs were immunopositive for GATA4. Cells counterstained with Hoechst 33342. **c** Western blot analysis revealed the synthesis of neurotrophic factors of GDNF and VEGF by SC. β-Actin is used as a control
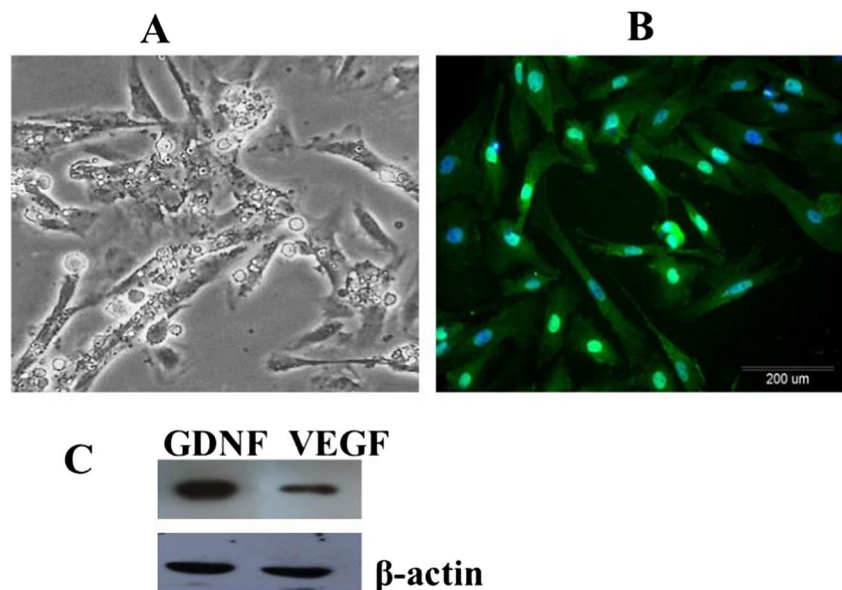
Fig. 2 Examination of PC12 neuritogenesis under oxidative stress. **a, b** Incubation of H_2O_2-treated PC12 cells with SC-CM for 24 h significantly decreased neurite outgrowth perturbation. Magnification: × 10. $^{###}P < 0.001$, representing the difference between the H_2O_2-treated group and control; $^*P < 0.05$, showing the difference between the SC-CM-treated H_2O_2 and H_2O_2 groups. The values are expressed as means ± SEM ($n = 5$)
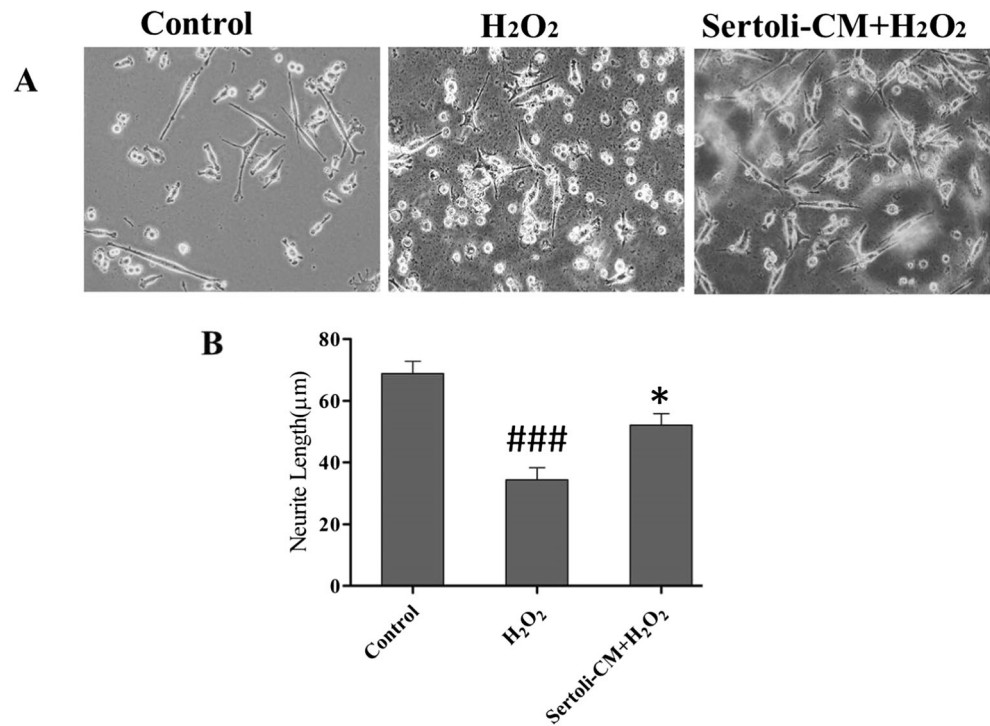

SC Implantation Diminished the Expression of Inflammatory Cytokines

The expression levels of genes related to inflammatory cytokines (TNF-α, IL-1β) were determined in the striatum 30 days after SC transplantation. The real-time qPCR results displayed that upregulation of inflammatory cytokines in the striatum was higher in the 3-NP + vehicle group in comparison to the control ($P < 0.001$). However, the expression level of TNF-α and IL-1β dropped noticeably in the SC + 3-NP group compared to the 3-NP + vehicle group (Fig. 11).

Fig. 3 The neuroprotective effect of conditioned media of SC (SC-CM). **a** PC12 cells were exposed to superoxide-induced oxidative stress, incubated with SC-CM for 24 h, then the number of live and dead cells (green and red fluorescents, respectively) was counted. **b** Viability of H_2O_2-treated PC12 cells in the presence of SC-CM measured by MTT assay, indicating the neuroprotection of PC12 cells under oxidative stress by SC-CM treatment. Scale bar = 10 μm. $^{###}P < 0.001$, exemplifying the difference between the H_2O_2-treated group and control; $^{***}P < 0.001$, showing the difference between the SC-CM-treated H_2O_2 and H_2O_2 group. The values are expressed as means ± SEM ($n = 5$)
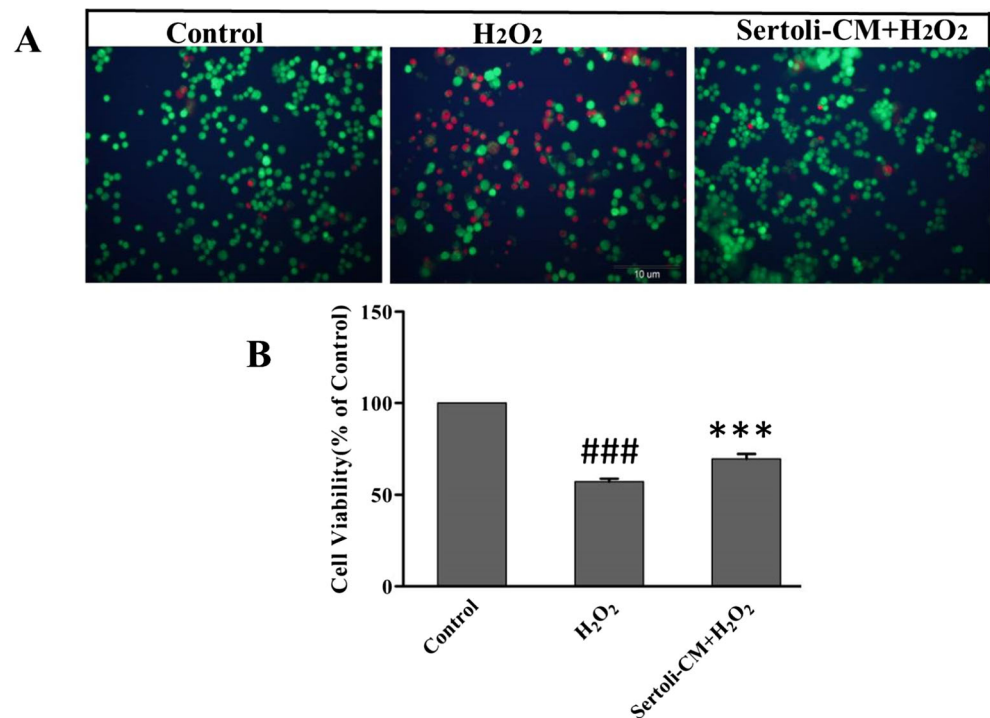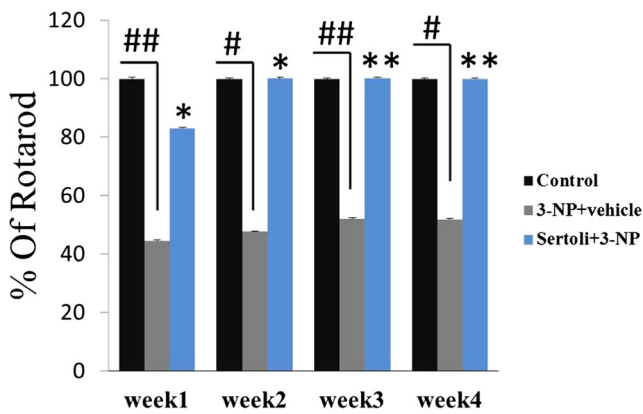
Fig. 4 Rotarod test in rats pre-treated with 3-NP. The SC + 3-NP group exhibited better rotarod performance compared to the 3-NP group. [#]$P < 0.05$ and [##]$P < 0.01$, representing the difference between the 3-NP group and control; *$P < 0.05$ and **$P < 0.01$, pointing to the difference between the SC + 3-NP group and 3-NP group. The values are expressed as means ± SEM ($n = 5$)

Discussion

This study assessed the restorative effects of SC and SC-CM on the 3-NP model of HD and PC12 cell line, respectively. According to our findings, the CM of GATA4-positive SC hindered H_2O_2-induced PC12 cell death and also grafted SC augmented both motor function impairment and striatal atrophy linked with HD.
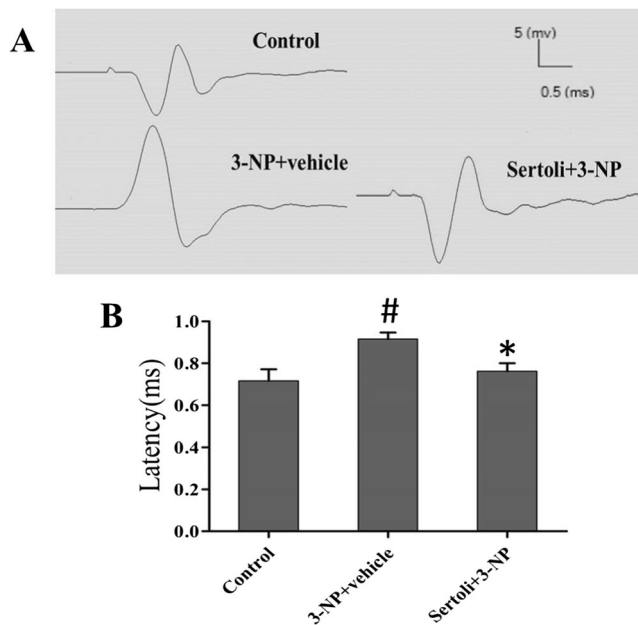

Fig. 5 Muscle activity in rats pre-treated with 3-NP. **a** The sciatic nerve was stimulated, and the muscle action potential was recorded in the gastrocnemius muscle. **b** Latency was measured in the control, 3-NP, and SC + 3-NP groups. Transplanted SC improved muscle activity in rats pretreated with 3-NP. Latency showed a significant reduction in the SC + 3-NP group contrary to the 3-NP group. [#]$P < 0.05$, representing the difference between the 3-NP group and control; *$P < 0.05$, pointing to the difference between the SC + 3-NP group and 3-NP group. The values are expressed as means ± SEM ($n = 5$)
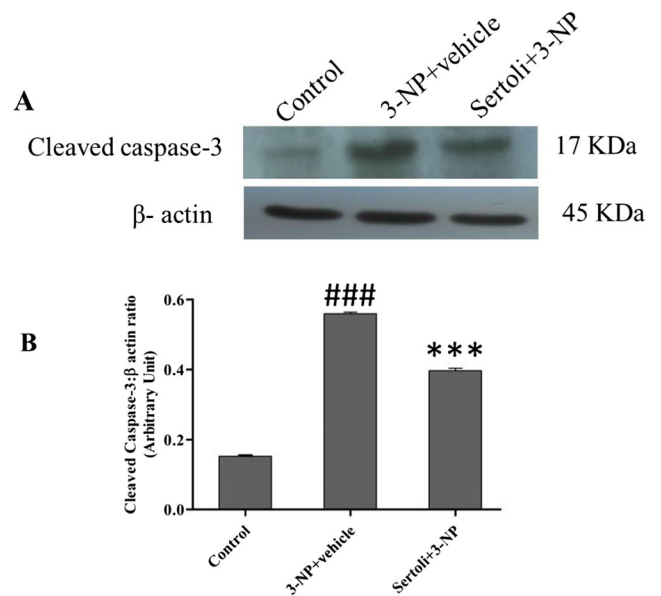

Fig. 6 Western blot analysis to evaluate the effect of transplanted SC on the expression level of an apoptotic marker caspase-3 in 3-NP-injected rats. **a** Western blots for cleaved caspase-3 are shown. Equal amounts of total proteins were separated by SDS-PAGE, and blots were probed with anti-caspase-3 and anti-β-actin antibody. The results showed high expression of cleaved caspase-3 in 3-NP-injected rats. **b** The densities of cleaved caspase-3 bands were measured, and their ratios to β-actin bands were calculated. [###]$P < 0.001$, indicating the difference between the 3-NP-injected group and control; ***$P < 0.001$, showing the difference between the SC + 3-NP group and 3-NP group

Cell transplantation therapy provides a promising approach for neurodegenerative diseases, and cell candidates with immunosuppression and trophic properties along with no ethical concerns are highly demanded, which aimed at implantation purposes (Boroujeni and Gardaneh 2017). Previous report showed the behavioral recovery of parkinsonian rats due to the trophic capabilities of single SC transplantation (Sanberg et al. 1997a; Borlongan et al. 1997). In our investigation, we used the 3-NP chemical model since firstly, this neurotoxin could appropriately present various
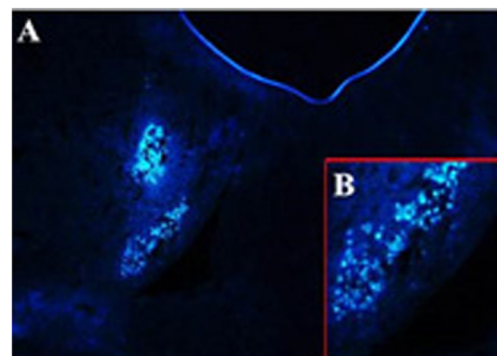

Fig. 7 Examination of striatal transplantation of SC. **a** Hoechst/DiI-labeled SC implanted in the striatum of 3-NP-lesioned rats survived after 30 days. Magnification: × 10. **b** Higher magnification of **a**

Fig. 8 The assessment of dendritic length of the striatum. **a** The silver staining of striatal medium spiny neuron (MSN) dendritic length in different groups. Magnification: × 10. **b** The striatum of the SC + 3-NP group revealed higher dendritic length compared with the 3-NP group. $^{###}P < 0.001$, demonstrating the difference between the 3-NP group and control; $^*P < 0.05$, displaying the difference between the SC + 3-NP group and 3-NP group. The values are expressed as means ± SEM ($n = 5$)
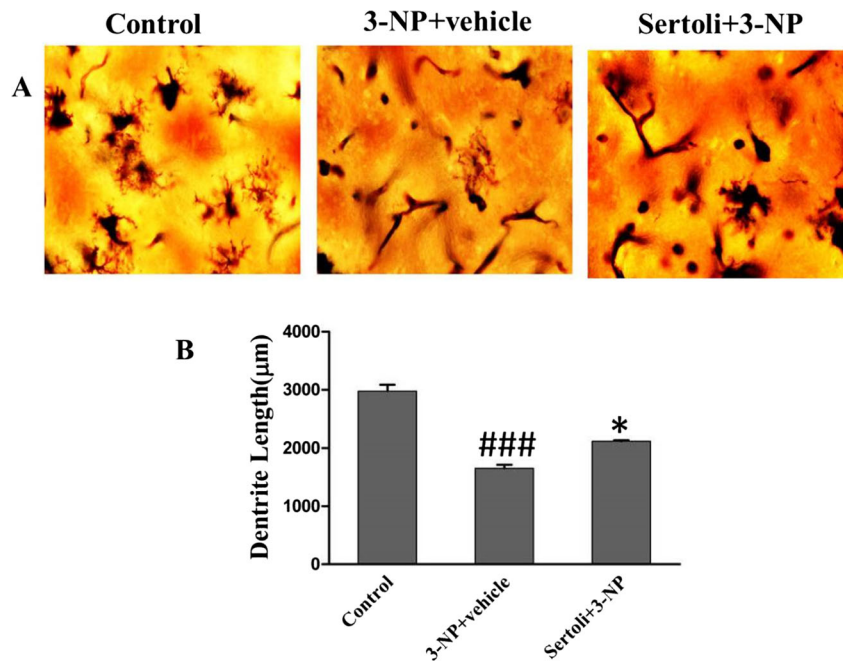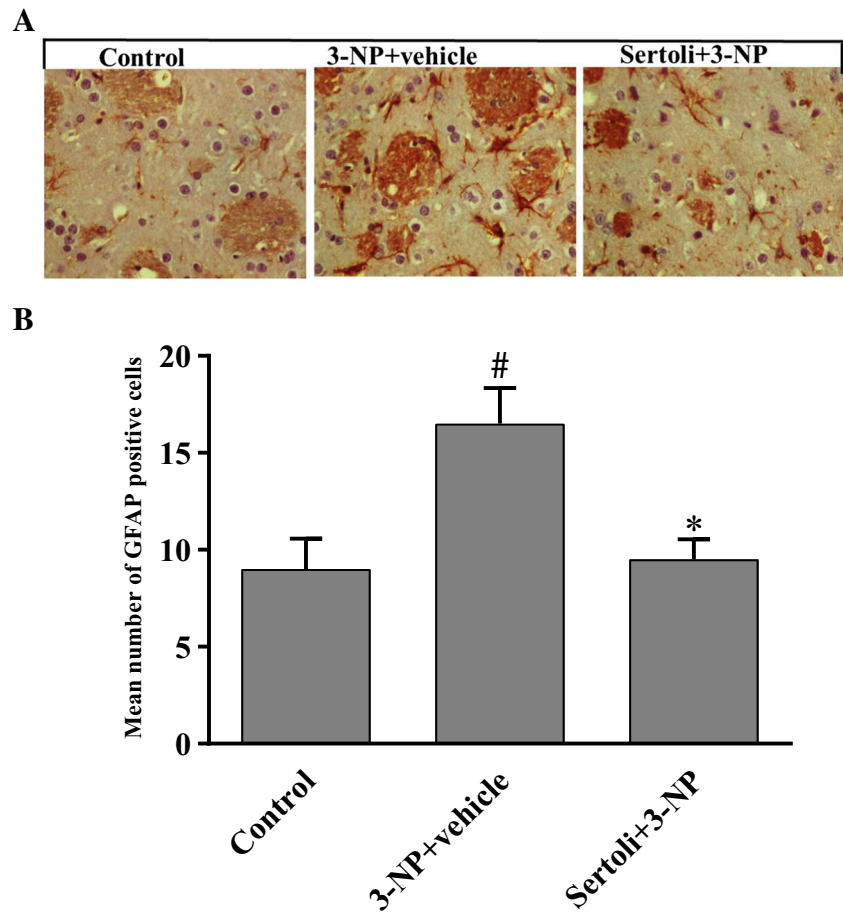
stages of HD through maneuvering time course of 3-NP (Borlongan et al. 1995), and secondly, it implemented its neurotoxicity by stimulation of oxidative stress in the striatum, followed by excessive reactive oxygen species (ROS) generation (Kumar et al. 2010), therefore facilitating the comparison of our in vitro and in vivo findings.

Fig. 9 Astrocytic migration (gliosis). **a** Immunohistochemistry against GFAP was done among various groups. Magnification: × 40. **b** Grafted SC in 3-NP-lesioned rats declined gliosis. $^#P < 0.05$, demonstrating the difference between the 3-NP group and control; $^*P < 0.05$, displaying the difference between the SC + 3-NP group and 3-NP group. The values are expressed as means ± SEM ($n = 5$)

A

B

Fig. 11 Transplant of SC declined the gene expression of inflammatory cytokines (TNF, IL-1β) as shown by real-time quantitative PCR ($*P < 0.05$); ($***P < 0.001$)
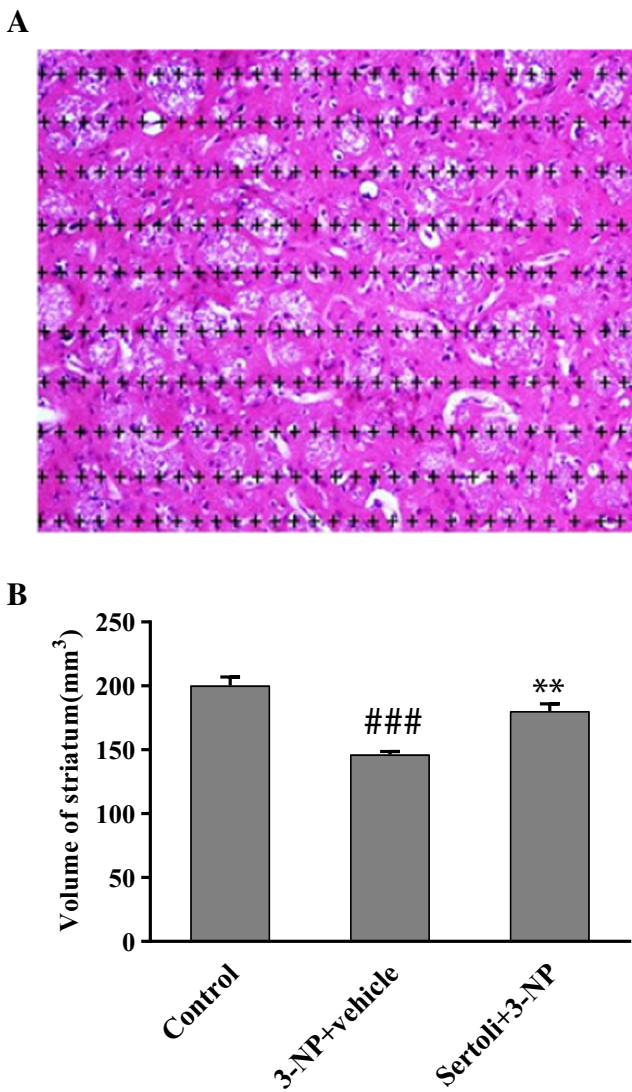
Fig. 10 Stereological analysis of striatal volume. **a** A grid of points was superimposed on the image of hematoxylin and eosin (H&E)-stained brain section in order to calculate the striatal volume. Magnification: × 4. **b** The volume of the striatum in the SC + 3-NP group showed an increase opposed to that in the 3-NP group. $^{###}P < 0.001$, demonstrating the difference between the 3-NP group and control; $**P < 0.01$, displaying the difference between the SC + 3-NP group and 3-NP group. The values are expressed as means ± SEM ($n = 5$)

SCs possess the capability to release several immunomodulators which may exert its impact after the transplantation in the recipient especially in case of allo- or xenogeneic engraftment (Chiappalupi et al. 2016). In an earlier report, SCs prolonged the survival of co-transplanted cells without the use of immunosuppressive drugs through decreasing microglial activation (Sanberg et al. 1997a). Moreover, several lines of evidences indicated that SCs provided neuroprotection for co-transplanted neuronal or non-neuronal cells, accompanied by enhancing the proliferation rate (Willing et al. 1999a; Willing et al. 1999b). In addition, SCs ameliorated the striatal atrophy in rodent models of Parkinson's disease
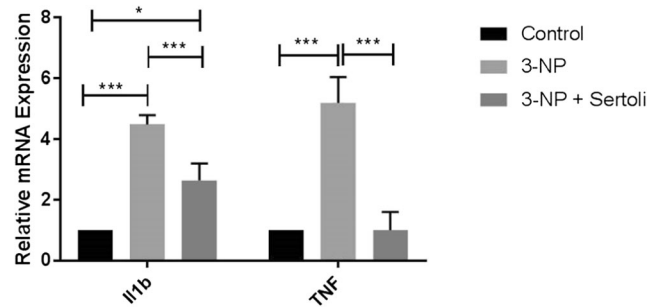
(Emerich et al. 2003). This was in line with our lab observations that implanted SC improved striatal volume in HD rats.

We detected the expression of neurotrophic factors such as GDNF and VEGF at the protein level in SC. Additionally, the presence of GDNF in reproductive organs could indicate a non-neuronal role for GDNF in these organs, perhaps in the differentiation of early germ cell precursors and/or in the maturation of accessory cells (Johnston et al. 2011). GDNF supports the survival and outgrowth of dopamine neurons following transplantation (Johasson et al. 1995). Moreover, in a pioneering investigation to verify the physiological trophic role for GDNF, it had been shown the extensive expression of GDNF messenger RNA (mRNA) in peripheral organs (Trupp et al. 1995). Also, GDNF had been implicated in the regulation of dopaminergic differentiation (Hynes and Rosenthal 1999) and it was elucidated to be the most potent neuroprotective agent on dopamine neurons in many model systems (Lin et al. 1993; Rosenblad et al. 2000; Kirik et al. 2001). Previously, it was shown that SC secreted GDNF and promoted the survival of grafted dopaminergic neurons. Likewise, GDNF played a substantial role in dopaminergic neuron differentiation when primate embryonic stem cells were co-cultured with SC (Yue et al. 2006). Further, based on an investigation, GDNF was not necessary for the induction of dopaminergic neurons (Buytaert-Hoefen et al. 2004).

Similar to our investigation, it was shown that caspase-3 was not activated in SC under apoptosis-inducing chemicals, whereas high expression rates of anti-apoptotic BCL2 family members were detected at both mRNA and protein levels (Aslani et al. 2017). Furthermore, we found that upon implantation of SC, the expression of pro-inflammatory cytokines showed an evident decline. This event proved to be attributed to the anti-inflammatory function of SC (Doyle et al. 2012). Thus, it is likely that the supporting environment provided by SC plays a vital role in regulating cell death pathways.

In conclusion, testis-derived SC, with immunoprivileged capacities could be employed in co-implantation platforms and/or using optimal gene delivery approaches, genetically engineered to deliver the functional genes in neurodegenerative diseases like HD (Mital et al. 2010; Boroujeni and Gardaneh

2018). We demonstrated that intrastriatally transplanted SC ameliorated degenerated striatum, reduced astrogliosis, and restored the overall motor skills. Nonetheless, further examinations regarding the immunoprotection of SC would pave the way for cell therapy approaches in clinical setting.

Compliance with Ethical Standards

Conflict of Interest The authors declare that they have no competing interests.

Ethical Approval All procedures performed in this study involving animals were in accordance with the ethical standards of the ethics committee of Shahid Beheshti University of Medical Sciences and under approval no. IR.SBMU.MSP.REC.1396.604.

References

Aslani F, Sebastian T, Keidel M, Fröhlich S, Elsässer HP, Schuppe HC, Klug J, Mahavadi P, Fijak M, Bergmann M, Meinhardt A, Bhushan S (2017) Resistance to apoptosis and autophagy leads to enhanced survival in Sertoli cells. Mol Hum Rep 23:370–380

Bates G, Tabrizi S, Jones L (eds) (2014). Huntington's disease (No. 64). Oxford University Press, UK

Borlongan CV, Koutouzis TK, Freeman TB, Cahill DW, Sanberg PR (1995) Behavioral pathology induced by repeated systemic injections of 3-nitropropionic acid mimics the motoric symptoms of Huntington's disease. Brain Res 697:254–257

Borlongan CV, Cameron DF, Saporta S, Sanberg PR (1997) Intracerebral transplantation of testis-derived Sertoli cells promotes functional recovery in female rats with 6-hydroxydopamine-induced hemiparkinsonism. Exp Neurol 148:388–392

Boroujeni ME, Gardaneh M (2017) Umbilical cord: an unlimited source of cells differentiable towards dopaminergic neurons. Neur Reg Res 12:1186

Boroujeni ME, Gardaneh M (2018) The superiority of sucrose cushion centrifugation to ultrafiltration and PEGylation in generating high-titer lentivirus particles and transducing stem cells with enhanced efficiency. Mol Biotechnol 60:185. https://doi.org/10.1007/s12033-017-0044-5

Buytaert-Hoefen KA, Alvarez E, Freed CR (2004) Generation of tyrosine hydroxylase positive neurons from human embryonic stem cells after coculture with cellular substrates and exposure to GDNF. Stem Cells 22:669–674

Chiappalupi S, Luca G, Mancuso F, Madaro L, Fallarino F, Nicoletti C, Calvitti M, Arato I, Falabella G, Salvadori L, di Meo A, Bufalari A, Giovagnoli S, Calafiore R, Donato R, Sorci G (2016) Intraperitoneal injection of microencapsulated Sertoli cells restores muscle morphology and performance in dystrophic mice. Biomaterials 75: 313–326

Clelland CD, Barker RA, Watts C (2008) Cell therapy in Huntington disease. Neurosurg Focus 24:E9

Cudicini C, Kercret H, Touzalin AM, Ballet F, Jégou B (1997) Vectorial production of interleukin 1 and interleukin 6 by rat Sertoli cells

cultured in a dual culture compartment system. Endocrinology 138:2863–2870

Doyle TJ, Kaur G, Putrevu SM, Dyson EL, Dyson M, McCunniff WT et al (2012) Immunoprotective properties of primary Sertoli cells in mice: potential functional pathways that confer immune privilege. Biol Reprod 86(6):1–14

Dufour JM, Dass B, Halley KR, Korbutt GS, Dixon DE, Rajotte RV (2008) Sertoli cell line lacks the immunoprotective properties associated with primary Sertoli cells. Cell Transplant 17:525–534

Emerich DF (2003) Sertoli cell grafts for Huntington's disease. An opinion. Neurotox Res 5:567

Emerich DF, Hemendinger R, Halberstadt CR (2003) The testicular-derived Sertoli cell: cellular immunoscience to enable transplantation. Cell trans 12:335–349

French LE, Hahne M, Viard I, Radlgruber G, Zanone R, Becker K, Müller C, Tschopp J (1996) Fas and Fas ligand in embryos and adult mice: ligand expression in several immune-privileged tissues and coexpression in adult tissues characterized by apoptotic cell turnover. J Cell Biol 133:335–343

Gnessi L, Emidi A, Jannini EA, Carosa E, Maroder M, Arizzi M, Ulisse S, Spera G (1995) Testicular development involves the spatiotemporal control of PDGFs and PDGF receptors gene expression and action. J Cell Biol 131:1105–1121

Griswold MD (1993) The Sertoli cell. Cache River, Clearwater 801p

Hemendinger R, Wang J, Malik S, Persinski R, Copeland J, Emerich D, Gores P, Halberstadt C, Rosenfeld J (2005) Sertoli cells improve survival of motor neurons in SOD1 transgenic mice, a model of amyotrophic lateral sclerosis. Exp Neurol 196:235–243

Hynes M, Rosenthal A (1999) Specification of dopaminergic and serotonergic neurons in the vertebrate CNS. Curr Opin Neurobiol 9:26–36

Johasson M, Friedemann M, Hopper B, Strömberg I (1995) Effects of glial cell line-derived neurotrophic factor on developing and mature ventral mesencephalic grafts in oculo. Exp Neurol 134:25–34

Johnston DS, Olivas E, DiCandeloro P, Wright WW (2011) Stage-specific changes in GDNF expression by rat Sertoli cells: a possible regulator of the replication and differentiation of stem spermatogonia. Biol Reprod 85:763–769

Kirik D, Georgievska B, Rosenblad C, Björklund A (2001) Delayed infusion of GDNF promotes recovery of motor function in the partial lesion model of Parkinson's disease. Eur J Neurosci 13:1589–1599

Korbutt GS, Elliott JF, Rajotte RV (1997) Cotransplantation of allogeneic islets with allogeneic testicular cell aggregates allows long-term graft survival without systemic immunosuppression. Diabetes 46:317–322

Kumar P, Kalonia H, Kumar A (2010) Huntington's disease: pathogenesis to animal models. Pharmacol Rep 62:1–14

Leegwater-Kim J, Cha JH (2004) The paradigm of Huntington's disease: therapeutic opportunities in neurodegeneration. NeuroRx 1:128–138

Lin LF, Doherty DH, Lile JD, Bektesh S, Collins F (1993) GDNF: a glial cell line-derived neurotrophic factor for midbrain dopaminergic neurons. Science 260:1130–1132

MacDonald ME, Christine M, Ambrose MP, Duyao RH, Myers CL et al (1993) A novel gene containing a trinucleotide repeat that is expanded and unstable on Huntington's disease chromosomes. Cell 72:971–983

Mital P, Kaur G, Dufour JM (2010) Immunoprotective Sertoli cells: making allogeneic and xenogeneic transplantation feasible. Reproduction 139:495–504

O'Bryan MK, Gerdprasert O, Nikolic-Paterson DJ, Meinhardt A, Muir JA, Foulds LM, Phillips DJ, de Kretser DM, Hedger MP (2005) Cytokine profiles in the testes of rats treated with lipopolysaccharide reveal localized suppression of inflammatory responses. Am J Physiol Regul Integr Comp Physiol 288:R1744–R1R55

Piccirillo CA, Chang Y, Prud'homme GJ (1998) TGF-β1 somatic gene therapy prevents autoimmune disease in nonobese diabetic mice. J Immun 161:3950–3956

Rodriguez AI, Willing AE, Saporta S, Cameron DF, Sanberg PR (2003) Effects of Sertoli cell transplants in a 3-nitropropionic

acid model of early Huntington's disease: a preliminary study. Neurotox Res 5:443–450

Rosenblad C, Kirik D, Björklund A (2000) Sequential administration of GDNF into the substantia nigra and striatum promotes dopamine neuron survival and axonal sprouting but not striatal reinnervation or functional recovery in the partial 6-OHDA lesion model. Exp Neurol 161:503–516

Sanberg PR, Borlongan CV, Saporta S, Cameron DF (1996) Testis-derived Sertoli cells survive and provide localized immunoprotection for xenografts in rat brain. Nat Biotech 14:1692–1695

Sanberg PR, Borlongan CV, Othberg AI, Saporta S, Freeman TB, Cameron DF (1997a) Testis-derived Sertoli cells have a trophic effect on dopamine neurons and alleviate hemiparkinsonism in rats. Nat Med 3:1129–1132

Sanberg PR, Saporta S, Borlongan CV, Othberg AI, Allen RC, Cameron DF (1997b) The testis-derived cultured Sertoli cell as a natural Fas-L secreting cell for immunosuppressive cellular therapy. Cell trans 6:191–193

Shamekh R, Mallery J, Newcomb J, Hushen J, Saporta S, Cameron DF, Sanberg CD, Sanberg PR, Willing AE (2006) Enhancing tyrosine hydroxylase expression and survival of fetal ventral mesencephalon neurons with rat or porcine Sertoli cells in vitro. Brain Res 1096:1–10

Shamekh R, Samuel S, Cameron DF, Willing AE, Sanberg CD, Johe K, Sanberg PR (2008) Effects of Sertoli cell-conditioned medium on ventral midbrain neural stem cells: a preliminary report. Neurotox Res 13:241–246

Skinner MK (1993) Secretion of growth factors and other regulatory factors. In: Russell LD, Griswold MD (eds) The Sertoli cell. Cache River, Clearwater, pp 237–248

Suarez-Pinzon W, Korbutt GS, Power R, Hooton J, Rajotte RV, Rabinovitch A (2000) Testicular Sertoli cells protect islet beta-cells from autoimmune destruction in NOD mice by a transforming growth factor-beta1-dependent mechanism. Diabetes 49:1810–1818

Trupp M, Rydén M, Jörnvall H, Funakoshi H, Timmusk T, Arenas E, Ibáñez CF (1995) Peripheral expression and biological activities of GDNF, a new neurotrophic factor for avian and mammalian peripheral neurons. J Cell Biol 130:137–148

Widenfalk J, Nosrat C, Tomac A, Westphal H, Hoffer B, Olson L (1997) Neurturin and glial cell line-derived neurotrophic factor receptor-β (GDNFR-β), novel proteins related to GDNF and GDNFR-α with specific cellular patterns of expression suggesting roles in the developing and adult nervous system and in peripheral organs. J Neurosci 17:8506–8519

Willing AE, Othberg AI, Samuel S, Anton A, Sinibaldi S, Poulos SG et al (1999a) Sertoli cells enhance the survival of co-transplanted dopamine neurons. Brain Res 822:246–250

Willing AE, Sudberry JJ, Othberg AI, Saporta S, Poulos SG, Cameron DF, Freeman TB, Sanberg PR (1999b) Sertoli cells decrease microglial response and increase engraftment of human hNT neurons in the hemiparkinsonian rat striatum. Brain Res Bull 48:441–444

Yang H, Al-Jazaeri A, Wright JR Jr (2002) The immunoprotective effect of Sertoli cells coencapsulated with islet xenografts is not dependent upon Fas ligand expression. Cell Transplant 11:799–801

Yue F, Cui L, Johkura K, Naoko Ogiwara N, Sasaki K (2006) Induction of midbrain dopaminergic neurons from primate embryonic stem cells by coculture with Sertoli cells. Stem Cells 24:1695–1706